

Vibratory Manipulation

Wesley H. Huang
Department of Computer Science
Rensselaer Polytechnic Institute
Troy, NY 12180

Abstract

Vibratory manipulation is the use of repeated impacts, typically at high frequency and low amplitude, to manipulate objects. Although this sort of manipulation is commonly used, e.g. in parts feeding systems, there has been relatively little work on formally analyzing the mechanics. In this paper, we focus on manipulating a planar slider repeatedly tapped by a vibrating manipulator. We find that there are two basic types of manipulation that can result: *intermittent tapping*, in which the object comes to rest in between impacts, and *continuous tapping*, in which the object remains in constant motion. Vibratory manipulation is often done by a manipulator with a fixed periodic motion; the resulting system can display chaotic behavior in the impact timing and amplitude. We examine the stability of the object motion and relate it to parameters of the manipulator vibration. Analytical results and simulated experiments are described to support our findings.

1 Introduction

Impulsive forces have many uses in manipulation. A vigorous strike to an object can move it very quickly from one place to another, or delicate taps can be used to precisely position it. We use the name *impulsive manipulation* to refer to any manipulation mode involving an impact with an object, followed by free motion of that object, subject to forces and constraints in its environment. Our focus in previous work (e.g. Huang and Mason 2000) was on tapping planar objects which then slide until they came to rest on a support surface.

In this paper, we investigate *vibratory manipulation* — manipulation using repeated impacts, typically at high frequency and low amplitude. Whereas impulsive manipulation primarily considers the mechanics of a single tap or a short sequence of taps, here we describe object behavior resulting from a large number of repeated impacts: the interaction between a vibrating striker and the mechanics governing object motion.

Vibratory manipulation is often used in industrial settings for parts feeding and singulation. One common example is the vibratory bowl feeder; the vibration causes parts in the bowl to climb up a spiral ramp along the inside wall of the device. Along this ramp are specially designed passive mechanical devices (e.g., “traps,” “wiper blades,” and “grooves”) that interact with the parts. These devices serve to filter parts in an undesired orientation by making them fall off the ramp, back to the bottom of the bowl. The vibration and design of the bowl feeder must be carefully tuned so that a stream of correctly oriented and singulated parts emerges at the top. Another example, the SONY APOS system employs a unique approach to parts feeding using trays with an array of “nests.” A tray is held at a slight tilt and vibrated while a stream of parts is poured over it. The shape of the nests and the vibration are tuned so that a part will remain in the nest only if it is in the correct orientation; it will otherwise be “kicked” out and slide off the tray. Though researchers have made some inroads into automating the design of these devices, manual design and tuning are still prevalent because of the complex interaction between parts and the manipulation devices.

The great promise of vibratory manipulation is that if, by proper mechanical design of a manipulator and choice of an open-loop vibratory motion, we can robustly perform a manipulation task, then a large number of parts can be manipulated in parallel. This paper aims to lay a foundation for understanding vibratory manipulation so that we can someday automatically design such systems.

1.1 Scope and assumptions

We limit our study in this paper to manipulating a slider on a planar surface. More specifically, we consider the general situation of manipulator with a vibrating tip: the manipulator follows a smooth trajectory while the tip executes some (small amplitude) periodic motion. The resulting object excitation is a series of small impacts at high frequency. The frequency and amplitude of the tip vibration may be specified as functions of the manipu-

lator trajectory or (when manipulating a single object) based on some feedback from the object motion.

We assume that the object is a thin extruded planar shape such that it is well approximated by planar analysis. The support surface is homogeneous, and Coulomb friction acts between the object and the surface. The impact between the object and manipulator is governed by the classical model of two-dimensional impact with Coulomb friction using Poisson’s hypothesis.

1.2 Objectives

There are three main questions that we will address in this paper:

1. *How can the gross behavior of an object under vibratory manipulation be characterized?* Instead of detailed calculations to extrapolate the result of a large number of taps, we want to succinctly characterize the constraints on object motion. In this paper, we will examine the resulting object motion for regular periodic striker motion superimposed on a constant velocity.
2. *How should vibratory manipulation be implemented?* Specifically, we will examine the relationship between the vibration frequency, the vibration amplitude, and the net striker speed for different modes of vibratory manipulation.
3. *What is the relationship between vibratory manipulation and pushing?*

1.3 Overview

We first examine one-dimensional vibratory manipulation in Section 2 in order to develop the basic ideas behind our analysis, and then proceed to the two-dimensional case in Section 3. In both sections, we:

- present a simple example that illustrates the basic issues of vibratory manipulation
- characterize the resulting object motion based on only the frequency and size of impulses (i.e., assuming any possible impulse can be applied at any desired frequency without regard to the manipulator)
- characterize manipulator parameters (e.g., frequency and amplitude of the vibration) that result in “stable” object-manipulator interaction.

In the one-dimensional case, the mechanics are very simple, making it easier to illustrate the difference between “continuous” and “intermittent” tapping. In addition, the interaction between the manipulator and the object is more clearly formulated in one dimension as a chaotic

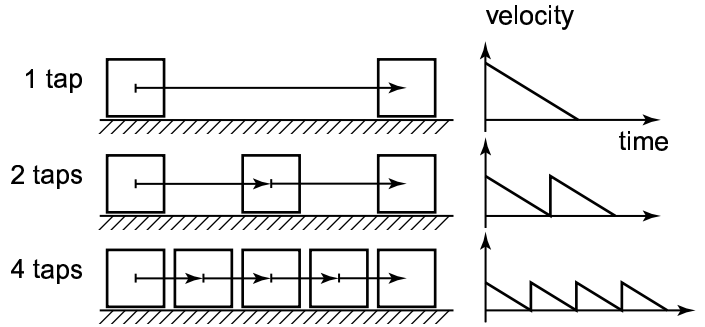


Figure 1: One-dimensional intermittent tapping.

system with stable modes determined by the manipulator parameters. In the two-dimensional case, these concepts still apply, but must be extended to address factors such as object rotation, manipulator shape, and numerical solutions to the equations of motion.

In order to address the relationship between vibratory manipulation and pushing, we consider the limiting cases — object motion when the frequency of taps increases and the amount of impulse approaches zero. We will show that continuous tapping becomes the same as pushing in the limit but that intermittent tapping has more restrictive motion constraints than pushing.

A review of related work appears at the end of the paper, before the conclusions.

2 One-dimensional analysis

We begin our analysis in one dimension to illustrate some of the basic characteristics of vibratory manipulation.

2.1 A simple task

Suppose we wish to move an object a certain distance along a straight line by tapping it. We could use a single tap that imparts the exact initial velocity for the object to slide and come to rest after traveling the required distance. However, this single large tap would be prone to large errors. Instead, we might use multiple small taps, letting the object come to rest after each tap. Each of these taps would be subject to a smaller error, and any error in one tap could be corrected in the next.

Suppose we are to translate the object a distance d using n identical taps. Before each tap, the object is at rest, and the tap produces a change in velocity of Δv . For now, we will disregard the manipulator and assume that we can deliver any desired impulse to the object at any time. Coulomb friction acts to slow the sliding object until it comes to rest, so the object decelerates at a constant

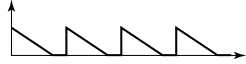
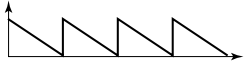


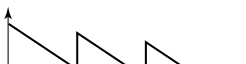
mode	pre-impact velocity	condition	velocity profile	characterization
intermittent	$v_0^- = 0$	$\Delta t > \frac{\Delta v}{\mu g}$		$\bar{v} = \frac{\Delta v^2}{2\mu g \Delta t}$
	$v_0^- = 0$	$\Delta t = \frac{\Delta v}{\mu g}$		$\bar{v} = \frac{\Delta v}{2}$
continuous	$v_0^- > 0$	$\Delta v = \mu g \Delta t$		$\bar{v} = v_0^- + \frac{\Delta v}{2}$
	$v_0^- > 0$	$\Delta v > \mu g \Delta t$		$\bar{a} = \frac{\Delta v}{\Delta t} - \mu g$
	$v_0^- > 0$	$\Delta v < \mu g \Delta t$		$\bar{a} = \frac{\Delta v}{\Delta t} - \mu g$

Table 1: Modes of vibratory manipulation in one dimension: the different modes are determined by the object pre-impact velocity v_0^- and the relationship between impulse train parameters Δv and Δt . The resulting motion can be characterized by the average velocity \bar{v} or average acceleration a .

rate of $-\mu g$, where μ is the coefficient of friction. After the tap, the object motion is described by:

$$\ddot{x}(t) = -\mu g \quad (1)$$

$$\dot{x}(t) = \Delta v - \mu g t \quad (2)$$

Let the time for the object to come to rest be $\Delta t = \Delta v / (\mu g)$.

The distance the object is to slide after the tap, $\frac{d}{n}$, is the integral of the velocity:

$$\frac{d}{n} = \int_0^{\Delta t} \dot{x} dt \quad (3)$$

This can be solved for the amount of time for the object to come to rest:

$$\Delta t = \sqrt{\frac{2d}{\mu g n}} \quad (4)$$

and for the required initial velocity:

$$\Delta v = \sqrt{\frac{2\mu g d}{n}} \quad (5)$$

Figure 1 illustrates this relationship for several values of n and shows the resulting velocity profiles.

2.2 Continuous versus intermittent tapping

In the example from the previous section, the manipulator provides a train of impulses, each of magnitude $M\Delta v$

and with a period Δt . There, Δt was chosen to be the time for the object to come to rest from an initial velocity Δv , and Δv was chosen based upon the number of taps n to cover a given distance d . In general, however, the manipulator could deliver train of (identical) impulses with arbitrary magnitude and period. In this section, we consider the object behavior resulting from arbitrary choice of Δv and Δt .

There are two distinct behaviors that can result: intermittent tapping, in which the object comes to rest after each tap, and continuous tapping, in which the object remains in constant motion. Table 1 illustrates these different behaviors and the corresponding conditions on the pre-impact velocity v_0^- and the relationship between the Δv and Δt parameters of the impulse train.

Under intermittent tapping, the exact timing of subsequent taps is not critical since the object comes to rest after each tap. However, as Δv decreases, the average velocity also decreases; using arbitrarily many small taps to cover a given distance will take an arbitrarily long time.

Under continuous tapping, the timing of impulses is important: the next tap must occur before the object comes to rest. The object will accelerate, decelerate, or remain at constant average velocity depending on whether tap provides a Δv that is larger, smaller, or equal to the lost velocity. One advantage of continuous tapping is that the parameters Δv and Δt can be adjusted so that the object maintains the same average velocity even as the size of the taps becomes arbitrarily small.

2.3 Manipulator interaction

We now consider the interaction between an object and a vibrating manipulator. Assume the manipulator follows a periodic motion superimposed on a constant velocity. Instead of the idealized impulse train of the previous section, here the amount of impulse delivered will vary, depending on exactly when when impact occurs. The timing of the impulse, in turn, will depend when the object, as it decelerates from the previous impact, comes into contact with the manipulator again.

We would like to characterize manipulator motions where the object follows some regular periodic motion, i.e., it impact the manipulator at the same phase of its motion every time. The point of characterizing when periodic object motion occurs may be to induce such motion, or it may be to *avoid* periodic motion! A study of vibratory parts feeders (Han and Lee 2002) showed that while feed rates are higher for periodic motion, with chaotic motion the feed rate is less sensitive to load, i.e., the number of parts on the feeder.

Periodic object motion should be stable — any variations should be automatically corrected so that the object remains in or near a regular periodic trajectory. For example, if the the object decelerates more slowly than expected, the impact will occur later than normal. In order to restore the impact to its normal time, the impact should impart a smaller impulse to the object.

In this section, we will assume the manipulator follows a sinusoidal motion superimposed on a constant velocity:

$$x_M(t) = \bar{v}t + A \sin 2\pi ft \quad (6)$$

where A and f are the vibration amplitude and frequency and \bar{v} is the (constant) average velocity. The interaction between the manipulator and object can be described by a discrete nonlinear system. By adapting results from an analogous system—a ball bouncing on a sinusoidally vibrating table—we can calculate manipulator parameters that result in stable periodic object motion.

2.3.1 Vibratory manipulation and ball bouncing

Suppose we observe the manipulator and the object in a reference frame moving at velocity \bar{v} . The manipulator trajectory is then a pure sinusoid:

$$v_M = A \sin 2\pi ft \quad (7)$$

If we assume that the object remains in continuous motion, then it is subject to a constant deceleration of μg due to friction. Figure 2 illustrates the trajectories of this system in the fixed and moving frames.

In the moving frame, the object and manipulator look exactly like a ball bouncing on a sinusoidally vibrating

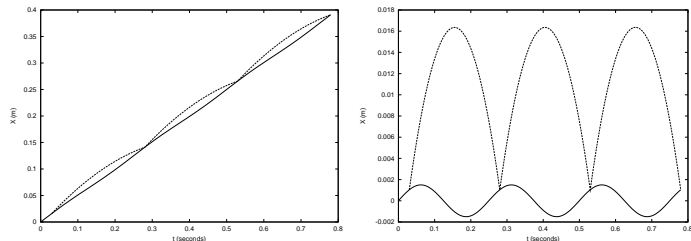


Figure 2: One-dimensional continuous vibratory manipulation: the left figure shows the object and manipulator trajectories in a fixed frame; the right, in a frame moving at the average manipulator velocity.

table. The difference is that the ball is pulled downwards by a constant gravitational force whereas the object is pulled “downwards” by a constant frictional force. The “bouncing ball problem” has been studied, both theoretically and experimentally, as an example of a nonlinear dynamic system. It has a number of stable periodic modes but can also display chaotic behavior. By applying results from the bouncing ball problem, we can characterize the vibration amplitude and frequency and the manipulator’s average velocity required to produce stable periodic object manipulation.

2.3.2 Analysis of vibratory manipulation

We will assume that the manipulator motion is not affected by impacts with the object. In practice, this might mean that the manipulator is much more massive than the object. Holmes (1982) studied the bouncing ball problem under approximated mechanics. He assumed that the vibration of the table is small compared to the displacement of the ball; therefore, the velocity of the ball before an impact is the same as its velocity after the previous impact, regardless of the exact time of impact. Bapat, Sankar, and Popplewell (1986) examined the exact mechanics and compared the approximated and exact mechanics. In the remainder of this section, we adapt Holmes’ analytic results to vibratory manipulation and report relevant observations by Bapat, Sankar, and Popplewell. We have adopted most conventions and notation of the latter work.

The “return map” of a discrete system maps the system state at one point in time to the state at the next point. For this problem, we consider a return map that maps the phase of the manipulator and the velocity of the object V before one impact to the phase and velocity before the next impact. Under the approximate mechanics, the return map can be used to show that for a coefficient of restitution less than 1, the trajectory of the ball will be bounded. Given the frequency f and amplitude A of the oscillation, the velocity of the object just

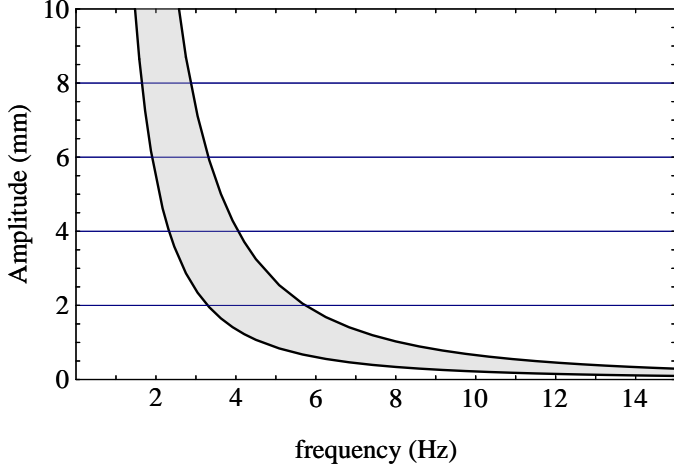


Figure 3: Relationship between frequency and amplitude of a sinusoidally vibrating striker required for (1, 1) vibratory manipulation for $e = 0.8$ and $\mu = 0.25$.

after an impact will eventually satisfy

$$|V| < \frac{(1+e)}{(1-e)} A 2\pi f \quad (8)$$

where e is the coefficient of restitution.

Fixed points of the return map correspond to different modes of stable periodic bouncing. These modes can be characterized by the designation (n, p) with n and p both positive integers, meaning that an impact occurs every n cycles of the manipulator oscillation with the object trajectory repeating after p impacts. We will only consider the simplest behaviors, $(n, 1)$ motions, in this section.

For a given n and f , stability analysis of the fixed points showed that in order to maintain stable periodic bouncing the amplitude of the manipulator must satisfy:

$$\frac{\mu g}{4\pi f^2} \frac{(1-e)}{(1+e)} n < A < \frac{\mu g}{4\pi f^2} \sqrt{\frac{(1-e)^2}{(1+e)^2} n^2 + \frac{1}{\pi^2}} \quad (9)$$

The velocity of the object after each impact is then:

$$V = \frac{\mu g n}{2f} \quad (10)$$

Note that the velocity is a function of n and f but not of A . Changing the amplitude of the oscillation changes the phase at which the impact occurs. The value of n is limited because V must satisfy Equation 8.

In addition, the average velocity of the manipulator must satisfy:

$$\bar{v} > V \quad (11)$$

so that the object remains in constant motion.

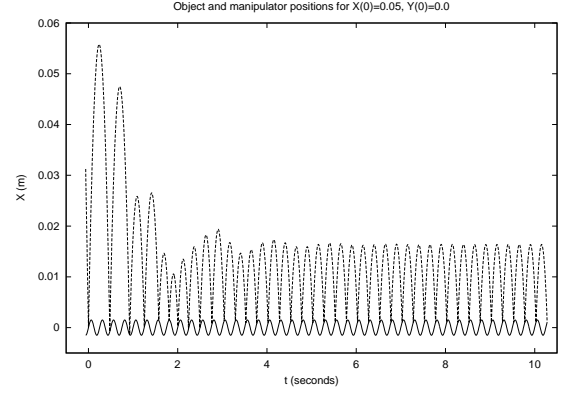


Figure 4: Object profile for linear tapping: the object trajectory and the sinusoidal manipulator motion are shown relative to the moving frame.

An example Suppose we take $n = 1$, $e = 0.8$, and $\mu = 0.25$. Equation 9 provides the following bound on the striker amplitude:

$$\frac{0.0217}{f^2} < A < \frac{0.0658}{f^2} \quad (12)$$

These bounds are shown in Figure 3. A manipulator amplitude below this range will result in decaying object amplitude. (See Figure 10 for a simulated example.) Increasing the amplitude above this range will result in period doubling, i.e. to $(2, 1)$ or $(1, 2)$ motions, and eventually to chaotic motion.

Figure 4 shows a simulated object trajectory for an object starting at rest and the initial impact occurring at a phase of 0° in the manipulator vibration.

2.3.3 Observations

Under periodic object motion, the object will move at the same average velocity as the manipulator. Since the analysis was done in the moving frame, stable periodic object motion can occur at any absolute velocity in the fixed frame.

Bapat, Sankar, and Popplewell (1986) found general agreement between the approximate and the exact mechanics (in particular, in the vibration amplitude bounds) when the coefficient of restitution is 0.8 or greater; at lower values there is some difference.

They also studied the regions of attraction for different stable periodic bouncing modes. Although limited in scope, their results are encouraging: they found that the regions of attraction for stable periodic modes are larger for the exact mechanics than they are for the approximate mechanics. The initial velocity of the ball is more influential than the initial phase in determining what mode the system settles into. A few additional results from other related work are reported in Section 5.

We note that if the object comes to rest before the next collision, then the object will appear, in the moving frame, to] follow the usual parabolic trajectory until its velocity decreases to $-\bar{v}$. This is the point at which the object comes to rest. It will then appear to “fall” at the constant velocity $-\bar{v}$ until it collides with the manipulator again. Though not amenable to analytic analysis (even under approximate mechanics), this intermittent tapping could be analyzed numerically to find manipulator parameters for stable periodic object motion.

3 Two-dimensional analysis

In two dimensions, there are two additional factors that come into consideration:

- rotation — in two dimensions, the object simultaneously translates and rotates. Because the force and torque due to friction are coupled, there is no analytic form for the velocity profiles, so we will generally have to rely upon numerical results.

The characterization of velocity and acceleration in the one-dimensional case (in Table 1) still applies, but we now characterize object motion by rotation centers which represent both translation and rotation.

- object shape — the shape of the object determines the contact normal at the impact point. As the object rotates, we must either “track” this point or choose a different contact point for each impact. For non-circular objects, a different contact point results in a different range of impulses that can be produced by impact.

In this section, we first give a summary of the mechanics of tapping in two dimensions. Due to the complexity of these mechanics, much of this section is restricted to considering circular axisymmetric objects, i.e. circular objects whose pressure distribution is a function of radius only. We then characterize object motion without regard to a manipulator and finally analyze the interaction between a vibrating manipulator and an object.

3.1 Mechanics of tapping

We will consider separately the mechanics of impact and that of a sliding object. The mechanics of tapping are a combination of the two.

3.1.1 Two-dimensional impact with friction

We use the classical model of two-dimensional impact with friction as described by Wang and Mason (1992) in

order to characterize the range of object velocities that is possible to produce by striking the object. After deciding upon the desired object velocities, it is fairly straightforward to calculate the parameters for a striker to produce these velocities through an impact.

One basic characteristic of the classical model is that the impulse delivered to the object must lie in a friction cone at the contact point. To be more precise, in the contact frame (where the y axis points into the object), the impulse will satisfy: $|P_x| \leq \mu P_y$. Any impulse within this friction cone can be produced by some striker velocity. This impulse leads to a change in the rotational and translational velocities of the object, $\Delta\omega$ and Δv , according to the relationship between the contact frame and the center of mass (COM) of the object.

Another property of this model is that the resulting $\Delta\omega$ and Δv can be scaled by scaling the impulse, and the impulse can be scaled by scaling the striker velocities relative to the object. When the pre- and post-impact velocity will be in the same direction, we are therefore only concerned with the ratio $\Delta\omega/\Delta v$. As it turns out, a continuous range of $\Delta\omega/\Delta v$ values can be produced by simply changing the angle of incidence of the striker.

For circular axisymmetric objects, the range of possible $\Delta\omega/\Delta v$ will be an interval that is symmetric about zero. This means that in the velocity space (v, ω) of a circular object sliding along a straight line, the possible changes in velocity can be represented by a cone pointing in the positive v direction (Huang 1997):

$$\frac{|\Delta\omega|}{\Delta v} \leq \frac{MR}{I\sqrt{1 + \frac{1}{\mu^2}}} \quad (13)$$

where M , I , and R are the mass, moment of inertia, and radius of the object, and μ is the coefficient of friction between the striker and the object.

3.1.2 Sliding objects with rotations

For objects with an axisymmetric pressure distribution, i.e. a pressure distribution $\rho(r)$ that is only a function of radius, the net force and torque load can be expressed as:

$$F\left(\frac{\omega}{v}\right) = \iint_A \mu g \hat{u}_x \rho(|\vec{r}|) da \quad (14)$$

$$T\left(\frac{\omega}{v}\right) = \iint_A \mu g |\vec{r} \times \hat{u}|_z \rho(|\vec{r}|) da \quad (15)$$

where $\vec{u} = \vec{v} + \hat{\omega} \times \vec{r}$ is the velocity at a point on the object. Note that the direction of the velocity, \hat{u} , is a function of the ratio $\frac{\omega}{v}$. It is simple to show that the net force in the \hat{u}_y direction is zero, so an axisymmetric object will slide in a straight line.

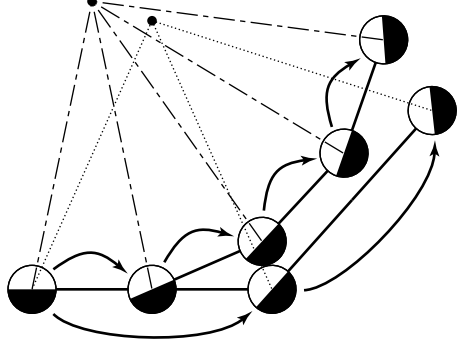


Figure 5: Scaling the impulse while tracking the same contact point results in motion about a different COR in two dimensions.

The equations of motion for a sliding axisymmetric object are:

$$-F\left(\frac{\omega}{v}\right) = m\dot{v} \quad -T\left(\frac{\omega}{v}\right) = I\dot{\omega} \quad (16)$$

where the initial object velocities are v_0 and ω_0 . The object will slide until it comes to rest at time t_f , and we are interested in the translation and rotation of the object:

$$x_f = \int_0^{t_f} v dt \quad \theta_f = \int_0^{t_f} \omega dt \quad (17)$$

Because the frictional force and torque load are functions of only $\frac{\omega}{v}$, trajectories can be scaled. If the initial velocities v_0 and ω_0 produce an object trajectory of $v(t)$ and $\omega(t)$, then the initial velocities kv_0 and $k\omega_0$ produce an object trajectory of $kv\left(\frac{t}{k}\right)$ and $k\omega\left(\frac{t}{k}\right)$. If the former produce a displacement of x_f and θ_f , then the latter produce a displacement of k^2x_f and $k^2\theta_f$.

We will characterize the motion of an object in two dimensions using a center of rotation (COR). The COR is the point about which the (net or instantaneous) motion of the object is a pure rotation. Note that since an axisymmetric object slides in a straight line, continuous motion about a COR is approximated with a series of straight line segments.

3.2 A simple task

Suppose a single tap moves an object (from rest) a distance x_f and produces a rotation of θ_f . We can accomplish this same displacement by using n taps, each delivering $1/\sqrt{n}$ of the impulse of the original tap. This is simple in the two-dimensional case because of the trajectory scaling property of the mechanics; we can simply scale the relative striker velocity while leaving its direction (relative to the object) the same. We assume that the contact point on the object is the same for all taps.

This seems identical to the one-dimensional introductory example in Section 2.1, but if we examine the object

motion (illustrated in Figure 5), we find that the object travels about a different COR for the smaller taps. If the initial velocity is along the positive x axis, then the COR is located at the point:

$$(x, y) = \left(\frac{x_f}{2n}, \frac{x_f}{2n \tan \frac{\theta_f}{2n}}\right) \quad (18)$$

and the radius of rotation about the COR is:

$$R = \frac{x_f}{2n \sin \frac{\theta_f}{2n}} \quad (19)$$

It is possible to make the object move about the same COR under different size taps, but this requires choosing a different contact point based on the magnitude of the impacts. For circular objects, this is a simple matter, but for arbitrarily shaped objects, this may not always be possible.

3.3 Intermittent versus continuous tapping

In the one-dimensional case, we considered a impulse train with an arbitrary Δv and Δt and classified the resulting object motion. There are two major differences between the one- and two-dimensional cases: the object motion cannot be determined analytically and not any $\Delta \vec{v}$ and $\Delta \omega$ can be produced by an impact with the object.

Since the object motion cannot be described analytically, there is no simple classification scheme to determine whether the object undergoes intermittent or continuous tapping and what its average velocity or acceleration is. Instead, we must numerically integrate the equations of motion. If Δt is long enough, the object comes to rest, resulting in intermittent tapping. Otherwise, we determine whether or not the impulse brings the velocities back to their original values — resulting in either constant average velocity or some acceleration or deceleration.

One way of visualizing continuous tapping in two dimensions is to consider the velocity space of the system. We illustrate using the velocity space (v, ω) of an axisymmetric object whose COM slides in a straight line as the object rotates. Figure 6 shows an example. From the object's initial velocities, the system evolves naturally until an impact occurs. The impact "kicks" the velocities up to some point within the cone described by Equation 13. If the impulse is in equilibrium with the velocity decay, i.e., the impulse brings the object velocities back to their initial values, then continuous tapping at constant average velocities results. Any other impulse results in net acceleration or deceleration of the translational or rotational velocities. This acceleration or deceleration could be constant, or it could decay, leading to an equilibrium cycle at some other initial object velocities.

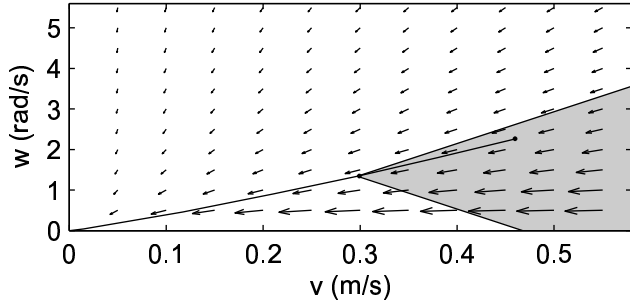


Figure 6: Velocity space for a sliding axisymmetric object with rotation. An example trajectory is shown; the “impact cone” is shown (shaded) at a point on this trajectory. Note that at this point, the object could be tapped to restore its initial velocities.

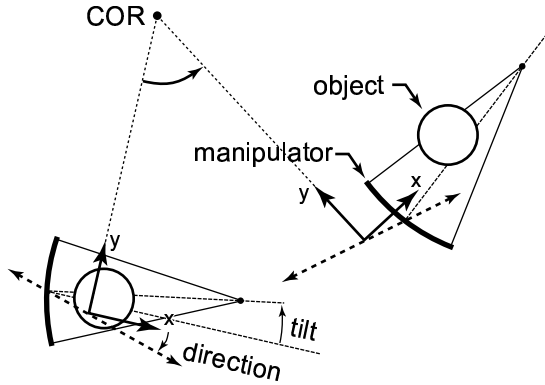


Figure 7: In two-dimensional vibratory manipulation, we use a striker frame that rotates about some center of rotation (COR). The striker may have a “tilt” angle relative to the striker frame x axis, and it oscillates along a line at a “direction” angle (along the dashed line).

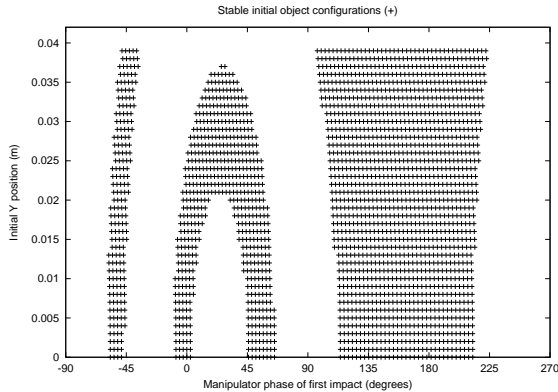


Figure 8: Stable initial configurations for linear tapping.

3.4 Manipulator interaction

In this section, we consider the interaction between the object and a manipulator that follows a prescribed motion: a periodic vibration superimposed on some smooth motion. In order to describe this motion precisely, we assume there is a “striker frame” which rotates about some COR on its y axis. The manipulator follows a linear sinusoidal motion relative to this frame. Note that the direction of the vibration need not be aligned with the x axis of the striker frame, and the manipulator may be tilted relative to this x axis. Figure 7 illustrates this situation. It is the vibration direction and manipulator tilt that allows an object to be tapped along a curved path.

We must also choose a shape for the manipulator since the object will contact the manipulator at different points. By using a convex shape, we can provide lateral stability — an impact that occurs on the left side of the manipulator should result in a restoring impulse that moves the object to the right. Here we will use a circular arc with a radius much larger than the (circular) object radius.

Like the one-dimensional case, the resulting system is similar to a ball bouncing on a sinusoidally vibrating plate. However, there are some significant differences. Besides object rotation and the nonanalytic form of the mechanics, the isotropy of Coulomb friction is another difference. Whereas in the bouncing ball problem, gravity acts only downwards, for two-dimensional vibratory manipulation, Coulomb friction acts to oppose object motion, whether it is “downward” or “sideways” (in the striker frame). This actually has the effect of increasing lateral stability because any side-to-side motion relative to the manipulator is damped.

We have conducted a number of simulations of two-dimensional vibratory manipulation. The frequency and amplitude relationship shown in Figure 3 is still approximately correct for two-dimensional tapping.

Our first set of simulations considered tapping in a straight line. For these simulations, the striker frame translates along the world x axis. The manipulator motion has a tilt and direction of 0° , i.e., the manipulator vibrates along the x axis, and the manipulator “faces” the positive x axis. The initial y position of the object was varied from 0 to 0.04 m, and the initial x position was varied so that the initial impact occurred from -90° to 270° in the manipulator vibration. Figure 8 shows the initial positions that resulted in stable periodic object motion. In these simulations, the object radius R is 5 cm, the manipulator is a 10 cm arc with a radius of curvature of 50 cm, the manipulator translational velocity is 0.5 m/s, the vibration amplitude is 1.5 mm, the vibration frequency is 4 Hz, the coefficient of friction is 0.2, and the coefficient of restitution is 0.8

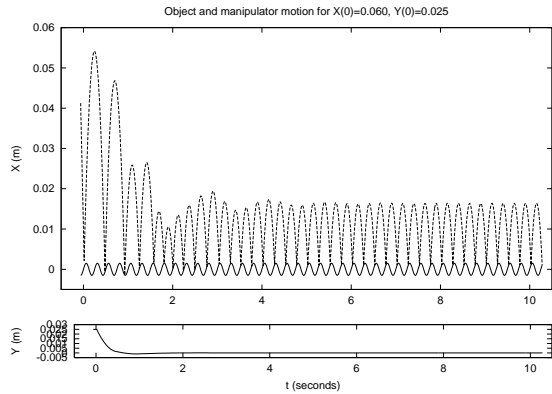


Figure 9: A stable profile for linear tapping. Here the object starts off the x axis.

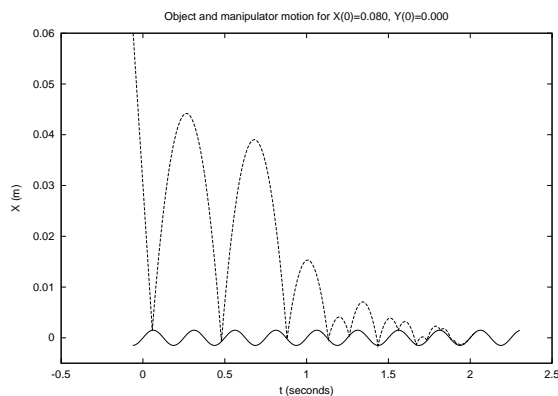


Figure 10: An unstable profile for linear tapping.

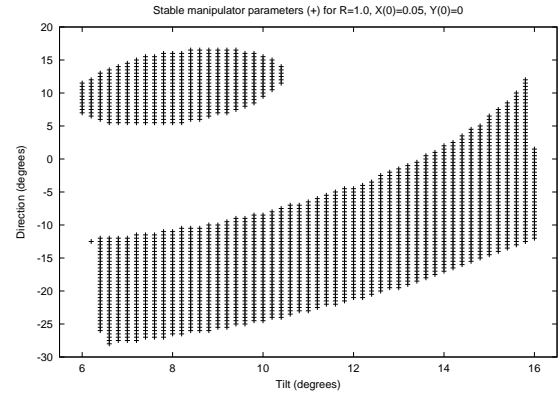


Figure 11: Stable configurations for rotational tapping.

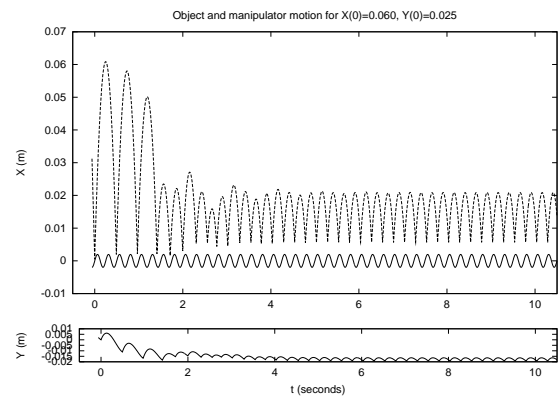


Figure 12: A stable profile for rotational tapping.

Figure 9 shows the object trajectory for one of the stable initial positions. Note the smooth decay of the y position to 0. For the unstable initial positions, the object comes to rest against the manipulator; Figure 10 shows one such object trajectory.

Our second set of simulations tested vibratory manipulation when the striker frame rotates about a finite COR. In these simulations, the striker frame follows a circular path with radius 0.5 m. The object always starts at the same position — so that the initial impact was at 0° in the manipulator vibration and with $y = 0$ in the striker frame at impact. The tilt of the manipulator and its vibration direction were varied.

Figure 11 shows the combination of “tilt” and “direction” angles that produce stable periodic object motion. For the unstable combinations, the object generally “rolled off” the manipulator as the striker frame rotated. Figure 12 shows the object trajectory for one of the stable set of parameters. Note the “bouncing” in the y coordinate of the object in striker frame, even in steady state; this is due to the rotation of the striker frame.

4 Comparison with pushing

As the frequency of taps increases and their amplitude decreases, vibratory manipulation may appear similar to pushing. However, there are motions under vibratory manipulation that cannot be done with a simple pusher. For example, the concave manipulator tapping a circular object, described in Section 3.4 can simultaneously rotate the object while translating the COM along a straight line.

In this section, however, we compare vibratory manipulation to pushing by comparing the range of instantaneous CORs that are possible under each mode of manipulation. These COR ranges essentially characterize how sharply an object can be turned. We derive the COR sets for intermittent and continuous vibratory manipulation in the limit — as the size of impacts approaches zero and the frequency approaches infinity — and compare them to the COR set for a single-point pusher acting on the same part.

4.1 Intermittent tapping in the limit

We start with Equation 18 which describes the COR location for a tap. We consider only 1 tap (i.e., $n = 1$) that produces a displacement of \vec{x}_f and θ_f , and rewrite this equation in vector form:

$$\frac{\vec{x}_f}{2} + \frac{\hat{z} \times \vec{x}_f}{2 \tan \frac{\theta_f}{2}} \quad (20)$$

Suppose we start with a tap that produces a finite displacement \vec{x}_f and θ_f under intermittent tapping. By scaling the relative striker velocities by a factor k , the initial object velocities are scaled by k , and the displacement is scaled by a factor k^2 . In the limit, the COR is then:

$$\lim_{k \rightarrow 0} \frac{k^2 \vec{x}_f}{2} + \frac{\hat{z} \times k^2 \vec{x}_f}{2 \tan \frac{k^2 \theta_f}{2}} = \lim_{k \rightarrow 0} \frac{\hat{z} \times k^2 \vec{x}_f}{2 \tan \frac{k^2 \theta_f}{2}} \quad (21)$$

Applying l'Hôpital's rule, we get

$$\lim_{k \rightarrow 0} \frac{\hat{z} \times \vec{x}_f}{\theta_f \sec^2 \frac{k^2 \theta_f}{2}} = \frac{\hat{z} \times \vec{x}_f}{\theta_f} \quad (22)$$

This limit will always exist as long as the original initial velocities can be achieved by tapping the object from rest.

A pure translation (COR at infinity) is always possible for a circular object. The distance to the closest COR is then determined by the minimum value of $\frac{x_f}{\theta_f}$ which corresponds to the maximum amount of rotation for a given translation distance. This is limited by maximum value of $\frac{\omega_0}{v_0}$ that can be produced by an impact to the object.

Let $b_{\min} = \frac{x_f}{\theta_f}$ for the maximum value of $\frac{\omega_0}{v_0}$ that satisfies Equation 13. The set of CORs for the limiting case of intermittent tapping is then:

$$\{\pm b \hat{z} \times \hat{v}_0 | b \in [b_{\min}, \infty)\} \quad (23)$$

4.2 Continuous tapping in the limit

As we decrease the amount of impulse delivered to the object with a tap under continuous tapping, the amount of time that the object slides, t_f , approaches zero. Starting with Equation 20, we get:

$$\lim_{t_f \rightarrow 0} \frac{\vec{x}_f}{2} + \frac{\hat{z} \times \vec{x}_f}{2 \tan \frac{\theta_f}{2}} = \lim_{t_f \rightarrow 0} \frac{\hat{z} \times \vec{x}_f}{2 \tan \frac{\theta_f}{2}} \quad (24)$$

By applying l'Hôpital's rule, we get:

$$\lim_{t_f \rightarrow 0} \frac{\hat{z} \times \frac{d}{dt_f} \int_0^{t_f} \vec{v} dt}{\frac{d}{dt_f} \int_0^{t_f} \omega dt} = \lim_{t_f \rightarrow 0} \frac{\hat{z} \times \vec{v}(t_f)}{\omega(t_f)} = \frac{\hat{z} \times \vec{v}_0}{\omega_0} \quad (25)$$

Thus, the COR in the limit is simply the initial (instantaneous) COR. This limit will always exist as long as the object can be tapped back to its initial starting velocities for all points within a neighborhood of its starting state.

We now consider the set of CORs possible for a circular axisymmetric object. A pure translation is always possible, corresponding to a COR at infinity. The closest COR will be determined by how much initial rotational velocity can be generated via a tap for a given amount of initial translational velocity.

We can determine a condition for the existence of the limit by considering the slope of the object trajectory in the velocity space. (See Figure 6 and Section 3.3.) A slope in this space is a change in rotational velocity divided by a change in translational velocity. The slope of the object velocity-space trajectory at the initial velocities is:

$$\frac{\frac{d\omega}{dt}}{\frac{dv}{dt}} = \frac{T(\frac{\omega_0}{v_0})/I}{F(\frac{\omega_0}{v_0})/M} \quad (26)$$

This slope must satisfy Equation 13 so that the initial velocities can be restored with a tap¹. Substituting and simplifying, we get:

$$\frac{|T(\frac{\omega_0}{v_0})|}{F(\frac{\omega_0}{v_0})} \leq \frac{R}{\sqrt{1 + \frac{1}{\mu^2}}} \quad (27)$$

If we let $1/c_{\min}$ be the largest value of $\frac{\omega_0}{v_0}$ that satisfies this equation, then the set of CORs for the limiting case of continuous tapping is:

$$\{\pm c \hat{z} \times \hat{v}_0 | c \in [c_{\min}, \infty)\} \quad (28)$$

¹When Equation 13 is satisfied by equality at $t = 0$, then it must be satisfied over the object trajectory for $t < \epsilon$ in order for the limit to exist.

4.3 Pushing

For pushing a circular object at a single point, a pure translation is always possible, corresponding to a COR at infinity. The closest COR depends on the object velocities that result in the maximum amount of (frictional) torque for a given amount of (frictional) force. Under quasistatic equilibrium, friction is balanced by the force applied by the pusher, and this force must lie in the friction cone at the contact point. This gives the constraint:

$$|T(\frac{\omega}{v})| \leq F(\frac{\omega}{v})R \sin(\tan^{-1} \mu) \quad (29)$$

which can be simplified to:

$$\frac{|T(\frac{\omega}{v})|}{F(\frac{\omega}{v})} \leq \frac{R}{\sqrt{1 + \frac{1}{\mu^2}}} \quad (30)$$

Note that this is the same as Equation 27, and therefore the set of CORs for pushing will be the same as for continuous tapping in the limit (Equation 28).

4.4 Discussion

Continuous tapping in the limit and pushing have identical constraints since Equations 27 and 30 are identical. These equations define c_{\min} , the distance to the closest COR for these manipulation modes.

The distance to the closest COR for the limiting case of intermittent tapping is b_{\min} which is defined by Equation 23. The relationship between b_{\min} and c_{\min} is:

$$b_{\min} = \frac{x_f(\frac{1}{c_{\min}})}{\theta_f(\frac{1}{c_{\min}})} \quad (31)$$

where $1/c_{\min}$ (a value of $\frac{\omega_0}{v_0}$) gets mapped through the sliding mechanics. In general, $b_{\min} > c_{\min}$, so intermittent tapping cannot generally “steer” an object as sharply as pushing or continuous tapping can. Also note that the analysis for intermittent tapping depends on the mechanics for axisymmetric objects, but that for continuous tapping and pushing can be applied to any object.

This limiting case analysis assumes infinitesimally small taps. For any finite approximation to these limiting cases, the set of possible CORs will, of course, be smaller.

5 Related work

There are a number of areas of related work, including parts feeding, impulsive and vibratory manipulation, and the ball bouncing problem.

5.1 Parts feeding

Since Boothroyd’s seminal work on characterizing industrial parts feeding systems (Boothroyd and Redford 1968; Boothroyd 1982; Boothroyd, Poli, and Murch 1992), there has been considerable interest in the robotics community in automating design of these systems. This section focuses on work related to design and analysis of parts feeders based on vibratory motion.

Berretty *et al.* (2001) describe an algorithm that can design traps (one type of filtering device in a vibratory bowl feeder) for planar polygonal parts. Christiansen, Edwards, and Coello Coello (1996) formulated a genetic algorithm to choose sequence of predesigned “gates” to orient a given part. Caine (1994) considers the configuration space of a part interacting with a feeder track to relate the shape of gates to the configuration of parts permitted to pass.

A number of researchers have developed tools to assist in the process of designing vibratory bowl feeders. Berkowitz and Canny (1996) applied an impulse-based dynamic simulator to determine a Markov model that characterizes the distribution of part poses. Maul and Thomas (1997) analyze the bowl vibration in conjunction with the contact mode of a part in order to predict the part velocity along the feeder track. Han and Lee (2002) have investigated chaotic and periodic modes of part motion along with the part contact modes in order to determine the feed rate. One of their results is that the feed rate can be higher for periodic part motion than for chaotic motion; however, it is more sensitive to the load (i.e., the number of parts in the feeder).

There are a few other approaches to parts feeding using vibrational motion that have been studied. Reznick and Canny (1998) demonstrated a system which uses planar translational and rotational vibrations to manipulate a number of parts on a single support surface simultaneously. Quaid (1999) developed a parts feeding approach where rotational vibratory motion is used to make parts ascend a spiral ramp.

The SONY APOS system (Hitakawa 1988), described in Section 1, is often cited as example of a real-world instance of a novel parts feeding system. Krishnasamy (1996) has done detailed study and analysis of this system to understand the underlying “entrapment” process.

5.2 Impulsive and vibratory manipulation

The first instance of impulsive manipulation in the robotics literature is a paper by Higuchi (1985) which describes the use of electromagnetic impulses for linear positioning of a metallic object.

Huang (1997) and Huang and Mason (2000) did for-

mal analysis of the mechanics, planning, and feedback control, along with experiments, for manipulating planar sliders via tapping. This work has complete mechanics only for objects with axisymmetric pressure distributions; Han and Park (2001) have addressed polygonal planar sliders. More recently, Li and Payandeh (2003) described an improved solution to the “inverse sliding problem,” the key problem in planning an impact to an object so it slides to a desired goal configuration.

One related mode of manipulation is the “releasing manipulation” of Zhu *et al.* (1996). Instead of using impact to impart initial object velocities, a manipulator smoothly accelerates the object and then releases it, letting it slide until it comes to rest. The mechanics of a planar slider are common to this work and the aforementioned work on tapping.

Another form of impulsive manipulation was demonstrated by Bishop and Spong (1999) and Partridge and Spong (1999) with their air-hockey playing robot. Though the sliding mechanics are quite different, impact plays a larger role in manipulating an air-hockey puck.

Aside from work on parts feeding systems, there has been relatively little work on vibratory manipulation. Yamagata and Higuchi (1995) built a piezoelectric actuator that delivers a small impulse to an object at frequencies up to many kilohertz. They have used this device for positioning optoelectronic elements and for positioning samples for an electron microscope (Yamagata *et al.* 1990). They have also explored the use of a thermal expansion as the motive force for this actuator (Yamagata *et al.* 1994) and have developed an optically excited version for micropositioning (Ohmichi, Yamagata, and Higuchi 1997).

5.3 The ball bouncing problem

As discussed in Section 2.3.2, Holmes (1982) and Bapat, Sankar, and Popplewell (1986) have studied the problem of a ball bouncing on a sinusoidally vibrating table. Their work, which we have applied to the analysis of one-dimensional vibratory manipulation, analyzes this problem both numerically and analytically under the exact mechanics and approximated mechanics.

Tuffillaro and Albano (1986) described an undergraduate experiment to build and observe the bouncing ball problem. They use a small steel ball bearing that bounces on a concave lens glued to a speaker. The speaker is driven by a sinusoidal waveform, and a piezoelectric film on the top of the lens produces a voltage impulse at every collision. They report experimentally observing (1, 1), (1, 2), (2, 1), and (1, 4) motions.

Schaal and Atkeson (1993) juggled a ping-pong ball using a “trampoline-like” racket. They observed that negative acceleration of the paddle trajectory at impact

seems to provide stability. They calculated the basin of attraction for periodic juggling to be 0.257 the area of the viable space of initial conditions. However, for a number of reasons (including mechanical variability and air resistance) the basin of attraction was significantly larger. In fact, they were unable to avoid getting a periodic (mostly period one) juggling pattern.

Wiesenfeld and Tuffillaro (1987) provide analysis to show how to suppress the period doubling behavior which could be applied to a vibratory manipulation system to maintain simple (1, 1) motions.

Bühler and Koditschek (1990) demonstrated a system that juggles a puck on an inclined plane using a bat. In order to achieve stable juggling, they developed a “mirror” control law which serves the bat to nonlinearly reflect the position of the puck. Using this sort of simple control law for vibratory manipulation is appealing but sensing the object would be difficult for high frequency, low amplitude motions.

6 Conclusions

In this paper, we have characterized the behavior of a planar slider under vibratory manipulation. This manipulation involves repeated impacts, typically with high frequency and low amplitude. There are two fundamental types of manipulation that can result: intermittent tapping, in which the object comes to rest in between impacts, and continuous tapping, in which the object is in continuous motion.

When the frequency and amplitude of a train of impulses is given, we can easily determine which mode of vibratory manipulation results. In the one-dimensional (translation only) case, it is simple to characterize the mode based on the impulse train. In two dimensions (with object rotation), we must simulate the object motion numerically to make this determination because of the complexity of the mechanics of a sliding rotating object.

In many applications for vibratory manipulation, the manipulator vibration is fixed, but the object does not receive a constant periodic train of impulses — the timing of one impact determines the magnitude of that impact, and the magnitude of this impact determines the timing of the next impact.

We therefore studied the interaction between a part and a manipulator with a fixed sinusoidal vibration superimposed on a constant smooth motion. In one dimension, we saw that this system is analogous to a ball bouncing vertically on a vibrating table. This is a well-studied chaotic system, and we adapted some of those results to characterize the relationship between the frequency and amplitude of the manipulator vibration and

stable periodic modes of the resulting object motion. In two dimensions, we ran simulations for a circular-arc shaped manipulator to characterize the manipulator parameters that result in stable periodic object motion.

We note that in applications of vibratory manipulation, it may be desirable to avoid periodic motion. With sufficient excitation, chaotic object motion can result from interaction with a manipulator with a constant periodic vibration. This could be used in a sort of simulated annealing in which the manipulator amplitude could be slowly decreased, and chaotic object motion would serve to “kick” the object out of local minima to reach a desired part configuration.

We discovered that continuous vibratory manipulation has the same basic motion constraints as pushing, but there are certain motions possible under vibratory manipulation that a simple pusher cannot do, such as rotating an object as its COM is translated along a straight line.

With further study, vibratory manipulation has the potential of enabling design of minimalist systems that can manipulate a large number of parts simultaneously. Ultimately, we should be able to design the shape of gates in a vibratory bowl feeder or nests of an APOS parts feeder, as well as pick an open-loop vibration so that interaction between the part and manipulator results in robust part manipulation.

Acknowledgments

This work was supported in part by the National Science Foundation under grant IIS-9977562.

References

- [1] C. N. Bapat, S. Sankar, and N. Popplewell. Repeated impacts on a sinusoidally vibrating table reappraised. *Journal of Sound and Vibration*, 108(1):99–115, 1986.
- [2] D. R. Berkowitz and J. Canny. Designing parts feeders using dynamic simulation. In *IEEE International Conference on Robotics and Automation*, pages 1127–1132, 1996.
- [3] R.-P. Berretty, K. Goldberg, M. H. Overmars, and A. F. van der Stappen. Trap design for vibratory bowl feeders. *International Journal of Robotics Research*, 20(11):891–908, November 2001.
- [4] B. E. Bishop and M. W. Spong. Vision-based control of an air hockey robot. *IEEE Control Systems Magazine*, 19(3):23–32, June 1999.
- [5] G. Boothroyd. *Assembly Automation and Product Design*. Marcel Dekker, 1992.
- [6] G. Boothroyd, C. Poli, and L. E. Murch. *Automatic Assembly*. Marcel Dekker, 1982.
- [7] G. Boothroyd and A. H. Redford. *Mechanized Assembly*. McGraw-Hill, 1968.
- [8] M. Bühler and D. E. Koditschek. From stable to chaotic juggling: Theory, simulation, and experiments. In *IEEE International Conference on Robotics and Automation*, pages 1976–1981, Cincinnati, OH, 1990.
- [9] M. Caine. The design of shape interactions using motion constraints. In *IEEE International Conference on Robotics and Automation*, pages 366–371, 1994.
- [10] A. D. Christiansen, A. D. Edwards, and C. A. Coello Coello. Automated design of part feeders using a genetic algorithm. In *IEEE International Conference on Robotics and Automation*, pages 1:846–851, 1996.
- [11] I. Han and Y. Lee. Chaotic dynamics of repeated impacts in vibratory bowl feeders. *Journal of Sound and Vibration*, 249(3):529–541, 2002.
- [12] I. Han and S.-U. Park. Impulsive motion planning for positioning and orienting a polygonal part. *International Journal of Robotics Research*, 20(3):249–262, March 2001.
- [13] T. Higuchi. Application of electromagnetic impulsive force to precise positioning tools in robot systems. In O. Faugeras and G. Giralt, editors, *International Symposium on Robotics Research: The Third International Symposium*. MIT Press, 1986.
- [14] H. Hitakawa. Advanced parts orientation system has wide application. *Assembly Automation*, 8(3):147–150, 1988.
- [15] P. J. Holmes. The dynamics of repeated impacts with a sinusoidally vibrating table. *Journal of Sound and Vibration*, 84(2):173–189, 1982.
- [16] W. H. Huang. *Impulsive Manipulation*. PhD thesis, Carnegie Mellon University, Aug. 1997. Available as Carnegie Mellon Robotics Institute technical report CMU-RI-TR-97-29.
- [17] W. H. Huang and M. T. Mason. Mechanics, planning, and control for tapping. *International Journal of Robotics Research*, 19(10):883–894, October 2000.
- [18] J. Krishnasamy. *Mechanics of Entrapment with Applications to Design of Industrial Parts Feeders*. PhD thesis, Massachusetts Institute of Technology, May 1996.

- [19] Q. Li and S. Payandeh. Planning velocities of free sliding objects for dynamic manipulations. In *IEEE International Conference on Robotics and Automation*, pages 3594–3599, 2003.
- [20] G. P. Maul and M. B. Thomas. A systems model and simulation of the vibratory bowl feeder. *Journal of Manufacturing Systems*, 16(5):309–314, 1997.
- [21] O. Ohmichi, Y. Yamagata, and T. Higuchi. Micro impact drive mechanisms using optically excited thermal expansion. *Journal of Microelectromechanical Systems*, 6(3):200–207, September 1997.
- [22] C. B. Partridge and M. W. Spong. Control of planar rigid body sliding with impacts and friction. *International Journal of Robotics Research*, 19(4):336–348, 1999.
- [23] A. E. Quaid. A miniature mobile parts feeder: Operating principles and simulation results. In *IEEE International Conference on Robotics and Automation*, pages 3:2221–2226, 1999.
- [24] D. S. Reznik and J. F. Canny. Universal part manipulation in the plane with a single horizontally-vibrating plate. In P. K. Agrawal, L. E. Kavraki, and M. T. Mason, editors, *Robotics: The Algorithmic Perspective*, pages 91–102. A K Peters, 1998.
- [25] S. Schaal and C. G. Atkeson. Open loop stable control strategies for robot juggling. In *IEEE International Conference on Robotics and Automation*, pages 3:913–918, Atlanta, GA, 1993.
- [26] N. B. Tufillaro and A. M. Albano. Chaotic dynamics of a bouncing ball. *American Journal of Physics*, 54(10):939–944, October 1986.
- [27] Y. Wang and M. T. Mason. Two-dimensional rigid-body collisions with friction. *ASME Journal of Applied Mechanics*, 59:635–641, Sept. 1992.
- [28] K. Wiesenfeld and N. B. Tufillaro. Suppression of period doubling in the dynamics of a bouncing ball. *Physica D*, 26(1–3):321–335, May-June 1987.
- [29] Y. Yamagata and T. Higuchi. A micropositioning device for precision automatic assembly using impact force of piezoelectric elements. In *IEEE International Conference on Robotics and Automation*, pages 666–671, 1995.
- [30] Y. Yamagata, T. Higuchi, N. Nakamura, and S. Hamamura. A micro mobile mechanism using thermal expansion and its theoretical analysis. In *IEEE Micro Electro Mechanical Systems: An Investigation of Micro Structures, Sensors, Actuators, Machines, and Robotic Systems*, pages 142–147, Oiso, Japan, Jan. 1994.
- [31] Y. Yamagata, T. Higuchi, H. Saeki, and H. Ishimaru. Ultrahigh vacuum precise positioning device utilizing rapid deformations of piezoelectric elements. *Journal of Vacuum Science & Technology A*, 8(6):4098–4100, November/December 1990.
- [32] C. Zhu, Y. Aiyama, T. Chawanya, and T. Arai. Releasing manipulation. In *IEEE/RSJ International Conference on Intelligent Robots and Systems*, volume 2, pages 2:911–916, Osaka, Japan, Nov. 1996.